AD NUMBER

AD420913

LIMITATION CHANGES

TO:

Approved for public release; distribution is unlimited.

FROM:

**Distribution authorized to U.S. Gov't. agencies and their contractors;
Administrative/Operational Use; OCT 1963. Other requests shall be referred to Aerospace Research Labs., Office of Aerospace Research, Wright-Patterson AFB, OH 45433.**

AUTHORITY

WL/DOA STINFO memo. dtd 18 Jul 1994

ARL 63-176

INVESTIGATIONS OF THE STEADY AND UNSTEADY MOTION OF FREELY FALLING DISKS

WILLIAM E. WILLMARTH
NORMAN E. HAWK
ROBERT L. HARVEY

THE UNIVERSITY OF MICHIGAN
ANN ARBOR, MICHIGAN

OCTOBER 1963

AEROSPACE RESEARCH LABORATORIES
OFFICE OF AEROSPACE RESEARCH
UNITED STATES AIR FORCE

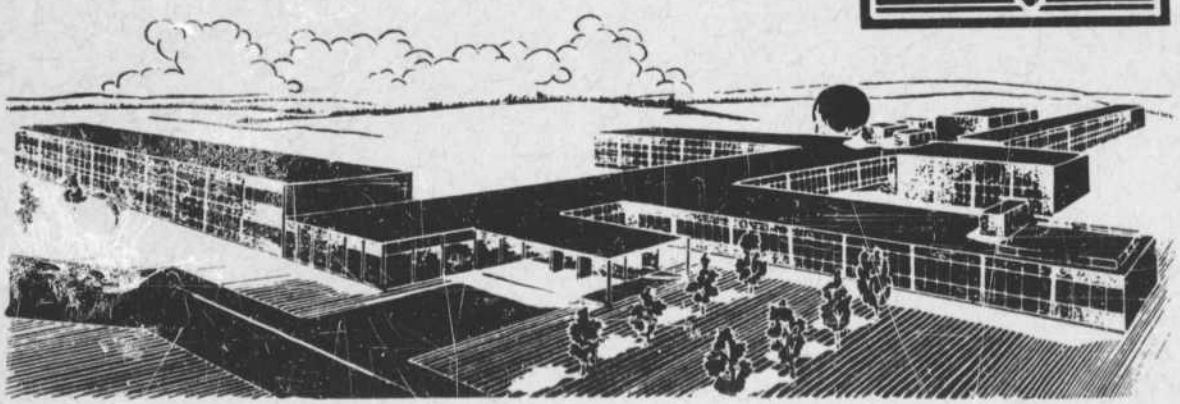

DISCLAIMER NOTICE

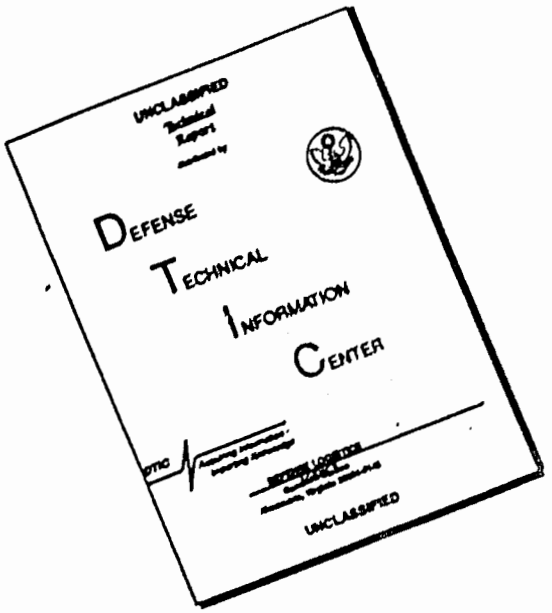

THIS DOCUMENT IS BEST QUALITY AVAILABLE. THE COPY FURNISHED TO DTIC CONTAINED A SIGNIFICANT NUMBER OF PAGES WHICH DO NOT REPRODUCE LEGIBLY.

NOTICES

When Government drawings, specifications, or other data are used for any purpose other than in connection with a definitely related Government procurement operation, the United States Government thereby incurs no responsibility nor any obligation whatsoever; and the fact that the Government may have formulated, furnished, or in any way supplied the said drawings, specifications, or other data, is not to be regarded by implication or otherwise as in any manner licensing the holder or any other person or corporation, or conveying any rights or permission to manufacture, use, or sell any patented invention that may in any way be related thereto.

- - - - - - - - - -

Qualified requesters may obtain copies of this report from the Defense Documentation Center, (DDC), Cameron Station, Alexandria, Virginia.

- - - - - - - - - -

DDC release to OTS not authorized

- - - - - - - - - -

Copies of ARL Technical Documentary Reports should not be returned to the Aerospace Research Laboratories unless return is required by security considerations, contractural obligations ot notices on a specific document

300 - October 1963 - 162-11-178

ARL 63-176

INVESTIGATIONS OF THE STEADY AND UNSTEADY MOTION OF FREELY FALLING DISKS

WILLIAM W. WILLMARTH
NORMAN E. HAWK
ROBERT L. HARVEY

THE UNIVERSITY OF MICHIGAN
DEPARTMENT OF AERONAUTICAL AND ASTRONAUTICAL ENGINEERING
ANN ARBOR, MICHIGAN

OCTOBER 1963

Contract AF 33(616)-7628
Project 7064
Task 7064-02

AEROSPACE RESEARCH LABORATORIES
OFFICE OF AEROSPACE RESEARCH
UNITED STATES AIR FORCE
WRIGHT-PATTERSON AIR FORCE BASE, OHIO

FOREWORD

This interim technical report was prepared by the personnel of the Department of Aeronautical and Astronautical Engineering, The University of Michigan, Ann Arbor, Michigan, under Contract AF 33(616)-7628 for the Aerospace Research Laboratories, Office of Aerospace Research, United States Air Force. The research reported herein was accomplished on Task 7064-02, "Research on Aerodynamic Stability Problems" of Project 7064, "Aerothermodynamic Investigations in High Speed Flow" under the technical cognizance of Mr. Otto Walchner of the Hypersonic Research Laboratory of ARL.

The authors wish to thank Professor A. M. Kuethe and Mr. Walchner for many helpful discussions. Gratitude is expressed to Mr. Robert Marcel, Mr. Patrick McSorley, and Mr. Fred Roos who helped conduct some of the tests.

ABSTRACT

The motions and wakes of freely falling disks have been studied and it has been found that the diverse motions of the disks exhibit a systematic dependence on the Reynolds number, Re, and the dimensionless moment of inertia, I*. The relation between I* and Re along the boundary separating stable and unstable pitching oscillations of the disk has been determined. The Reynolds number for stable motion of a disk with large I* is 100 in agreement with the Reynolds number for stability of the wake of a fixed disk. Slightly unstable disks of large I* were stabilized by reducing the moment of inertia. The highest Reynolds number for stable disk motion was 172. At higher Reynolds numbers the disks exhibited periodic pitching and translational oscillations. The laminar wake behind certain of the oscillating disks consisted of a staggered arrangement of two rows of regularly spaced vortex rings similar to the wake observed behind liquid drops by Margarvey and Bishop. The dependence of the dimensionless frequency of oscillation on I* and Re was determined along the boundary for stable motion and at higher Reynolds numbers when the wake was turbulent. Tumbling motions of the disks were observed when the Reynolds number was large $Re > 2000$ and I* was greater than a certain value, $I^* \doteq 10^{-2}$.

TABLE OF CONTENTS

LIST OF ILLUSTRATIONS

LIST OF TABLES

1. INTRODUCTION

The steady or unsteady motion of bodies with poor aerodynamic shapes cannot, at the present state of development of fluid mechanics, be calculated from the equations of motion for the flow. Therefore, our understanding of the fluid mechanical aspects of the body motion and flow field must rely on the results of systematic experimental investigations in which the significant parameters are varied over a wide range. This paper gives some results on various features of the steady and unsteady motion and flow over freely falling disks. The disk was chosen for these studies because when the flow is directed normal to the face of the disk, it represents an extreme example of a poor aerodynamic shape.

Some aspects of the flow field about a disk and other bluff bodies are already known. A summary of the known phenomena may be found in Goldstein.[1] At very low Reynolds numbers when the inertial forces of the fluid can be neglected and the flow is steady (Stokes flow) Oberbeck[2] has computed the drag coefficient and the flow field near the disk. At higher Reynolds numbers when inertial forces in the fluid first become important Oseen[3] has computed a correction term to the drag coefficient computed by Oberbeck. At Reynolds numbers above 100 the flow field in the wake becomes unstable and steady flow about the disk is no longer observed. In the case of two-dimensional bluff bodies a Karman vortex street[4] is developed in the wake. In three dimensions, where the geometry is more complicated, the wake flow is periodic,[5,6] but not as simple as the two-dimensional case, because the vorticity that appears in the wake is not aligned in one direction when it is formed. Rosenhead, in an appendix to Stanton and Marshall's report,[5] has given an excellent discussion of the possible eddy systems in the wake of circular disks. We shall refer to his discussion later in the paper. At higher Reynolds numbers the flow in the wake behind the body becomes turbulent. Roshko[7] has described the turbulent wake, which includes vestiges of the Karman vortex trail, for the case of two-dimensional bluff bodies. The three-dimensional turbulent wake structure is more complicated and has not been studied in as much detail as the two-dimensional turbulent wake. In the flow field and wake of a freely falling disk, one may expect to find vestiges of these phenomena. In addition, new phenomena that are caused by the motion of the disk as it moves about under the influence of the aerodynamic forces will appear.

We began the present investigation with the aim of identifying and understanding the more interesting and important features of the flow field and motion of a free disk. In our description of the unsteady phenomena we will be concerned primarily with the dimensionless parameters upon which the unsteady motion and flow field depend. After our investigation was well under way, we found the excellent paper of Schmiedel[8] in which many features of the steady and unsteady flow field and motions of freely falling disks and spheres are described. Schmiedel's work covers the range of Reynolds numbers from creeping motion up to Reynolds numbers of the order of 300. We will describe the flow phenomena using Schmiedel's results and ideas at low Reynolds numbers and add our new observations in the low Reynolds number range and at higher Reynolds numbers.

Manuscript released August, 1963, by the authors for publication as an ARL Technical Documentary Report.

2. EXPERIMENTAL APPARATUS

The experiments were performed by dropping disks made from materials of varying density into containers filled with tap water or with solutions of distilled water and glycerol. The disks were made from homogeneous metals or plastics whose specific gravity was greater than one. All the disks were made by machining thin sheets of the disk material on a high speed lathe. The disks were flat and the edges were square. The large disks were easily clamped on the rotating head stock with a rotating rubber pad mounted on the tail stock. Small thin disks were glued on the end of a rod clamped in a chuck. The glue used was Eastman 910 adhesive. In this way, very thin flat disks were made. The disks were removed from the rod with a razor blade and soaked in an Epoxy resin solvent until clean. The dimensions and density of the various disks were measured and are given in Tables I, II, and III.

The fluid containers were Plexiglas tubes of 11, 15, and 30 cm diam of various lengths. A square Plexiglas container 30 x 30 x 120 cm was used to photograph the disk motion and flow field. The effect of container size on the motion and flow field of the disks was appreciable only when large amplitude pitching oscillations were observed. These effects are discussed in Sections 3B, 3D, and 3E.

The rate of descent of the disks was obtained by stop watch measurements of the time required for the disk to fall a known distance. The frequency of disk oscillation was always low enough to allow the observer to measure an average frequency by counting the number of oscillations in a measured time interval. The temperature of the tap water was measured and its viscosity was obtained from the tables of Bingham and Jackson.[9] The specific gravity of the glycerol and distilled water solution was measured with a float type hydrometer. From the temperature and specific gravity of the glycerol and water solutions the coefficient of viscosity was obtained by interpolation from the tables published in the Handbook of Chemistry and Physics.[10] We have checked our experimental procedures and apparatus by comparing our drag coefficients with those measured by Schmiedel[8] for Reynolds numbers less than 100. The comparison is shown in Figure 5.

TABLE I

Disk Drag Coefficient Data at Low Reynolds Numbers in the Stable Region

Test No.	dx10(cm)	$t/dx10^3$	$\rho_2(g/cm^3)$	$\rho_1(g/cm^3)$	$\nu x10^2(cm^2/sec)$	U(cm/sec)	Re	C_D
1	3.18	12.0	7.84	1.20	31.2	1.55	1.58	17.3
2	3.18	10.0	7.84	1.18	11.4	2.91	8.10	4.16
3	7.62	3.3	7.84	1.17	19.0	2.95	11.8	3.25
4	7.62	3.3	7.84	1.16	15.3	3.15	15.7	2.88
5	15.2	1.67	7.84	1.18	28.5	3.07	16.4	2.97
6	7.62	3.3	7.84	1.15	11.6	3.54	23.2	2.30
7	15.2	1.67	7.84	1.17	19.0	3.63	29.1	2.14
8	25.4	1.0	7.84	1.18	28.5	3.79	33.8	1.95
9	31.8	10.0	7.84	1.12	3.96	4.47	35.9	1.86
10	7.62	3.3	7.84	1.13	6.95	4.05	44.4	1.78
11	7.62	3.3	7.84	1.12	5.48	4.41	61.3	1.54
12	5.08	5.0	7.84	1.09	3.12	4.62	75.0	1.44
13	3.18	10.0	7.84	1.08	2.14	5.05	74.8	1.52
14	15.2	1.67	7.84	1.13	6.66	4.62	106.0	1.38

TABLE II

Data for the Boundary Between Stable and Unstable Pitching Oscillations of a Disk

Test No.	dx10(cm)	t/dx10^3	ρ_2(g/cm^3)	ρ_1(g/cm^3)	νx10^2(cm^2/sec)	U(cm/sec)	Re	I*x10^3	Motion
1	6.35	42.0	7.84	1.15	8.36	14.1	107.0	14.1	U
2	6.35	42.0	7.84	1.15	8.95	14.2	101.0	14.0	B
3	6.35	42.0	7.84	1.16	9.56	14.6	97.3	14.0	SO
4	6.35	38.0	7.84	1.15	8.36	13.5	102.0	12.8	U
5	6.35	38.0	7.84	1.15	8.75	13.2	96.0	12.7	B
6	6.35	38.0	7.84	1.16	9.56	14.4	95.4	12.6	SO
7	3.18	32.0	7.84	1.07	2.25	9.53	134.0	11.4	U
8	3.18	32.0	7.84	1.09	3.12	10.2	103.0	11.2	B
9	6.35	30.0	7.84	1.14	7.10	12.2	109.0	10.1	U
10	6.35	30.0	7.84	1.14	7.22	11.9	104.0	10.1	B
11	6.35	30.0	7.84	1.15	8.36	12.2	93.0	10.0	SO
12	6.35	20.0	7.84	1.14	6.70	10.2	100.0	6.75	B
13	3.18	16.0	7.84	1.05	1.77	6.69	120.0	5.84	U
14	3.18	16.0	7.84	1.07	1.99	6.63	106.0	5.76	B
15	3.18	16.0	7.84	1.09	3.05	6.60	68.6	5.62	SO
16	3.18	76.0	1.24	1.00	1.00	3.22	102.0	4.60	SO
17	3.18	12.0	7.84	1.06	1.78	6.10	109.0	4.36	B
18	5.08	11.2	7.84	1.10	3.04	6.51	109.0	3.95	U
19	5.08	11.2	7.84	1.08	2.86	6.49	123.0	3.99	U
20	5.08	11.2	7.84	1.10	3.13	6.57	107.0	3.94	B
21	5.08	11.2	7.84	1.11	3.75	6.46	87.5	3.91	SO
22	5.08	10.0	7.84	1.10	3.21	6.63	112.0	3.51	B
23	5.08	8.85	7.84	1.07	2.52	5.69	115.0	3.14	U
24	5.08	8.85	7.84	1.07	2.50	5.46	111.0	3.12	B
25	5.08	8.85	7.84	1.08	2.80	5.55	101.0	3.11	SO
26	6.35	8.0	7.84	1.10	2.98	5.63	120.0	2.81	U
27	6.35	8.0	7.84	1.10	3.08	5.73	118.0	2.81	B
28	6.35	8.0	7.84	1.10	3.22	5.73	113.0	2.80	SO
29	25.4	1.0	7.84	1.14	7.88	4.81	155.0	0.34	SO

TABLE II (Concluded)

Test No.	dx10(cm)	t/dx10³	ρ_2(g/cm³)	ρ_1(g/cm³)	νx10²(cm²/sec)	U(cm/sec)	Re	I*x10³	Motion
30	25.4	1.0	7.84	1.14	7.68	4.84	160.0	0.34	B
31	25.4	1.0	7.84	1.14	6.98	4.48	163.0	0.34	U
32	15.2	1.67	7.84	1.11	4.33	4.76	158.0	0.52	SO
33	15.2	1.67	7.84	1.11	4.33	4.82	170.0	0.52	B
34	15.2	1.67	7.84	1.10	3.85	4.76	180.0	0.58	U
35	7.62	3.33	7.84	1.07	2.32	5.25	167.0	1.20	B
36	7.62	3.33	7.84	1.07	2.52	5.25	158.0	1.19	S
37	7.62	3.33	7.84	1.06	2.20	5.08	176.0	1.20	U
38	5.08	5.0	7.84	1.06	2.20	5.65	130.0	1.80	SO
39	5.08	5.0	7.84	1.05	1.84	4.92	136.0	1.84	U
40	7.62	6.66	7.84	1.11	4.11	6.62	123.0	2.30	SO
41	7.62	6.66	7.84	1.10	3.81	6.23	125.0	2.31	B
42	7.62	6.66	7.84	1.10	3.62	6.77	142.0	2.32	U
43	6.35	7.00	7.84	1.10	2.98	5.75	98.0	2.46	SO
44	6.35	7.00	7.84	1.08	2.38	5.75	123.0	2.50	B
45	6.35	7.00	7.84	1.07	2.16	5.69	134.0	2.51	U
46	10.2	2.50	7.84	1.08	2.83	3.00	184.0	0.89	U
47	10.2	2.50	7.84	1.08	2.68	4.76	180.0	0.89	U
48	10.2	2.50	7.84	1.09	2.92	4.93	172.0	0.88	B
49	10.2	2.50	7.84	1.08	2.83	3.25	170.0	0.89	SO
50	10.2	2.50	7.84	1.09	3.04	4.03	135.0	0.88	SO

TABLE III

Data for Regular Pitching Oscillations and for Tumbling Motion of Disks

Test No.	dx10(cm)	$t/dx10^2$	ρ_2(g/cm^3)	I^*x10^3	$\nu x10^3$(cm^2/sec)	U(cm/sec)	nd/Ux10	Re	C_D
1	2.53	6.6	1.14	3.71	10.4	5.06	4.00	1230	1.82
2	2.57	6.2	1.30	3.98	10.4	5.85	3.95	1440	2.77
3	2.54	6.9	1.69	5.73	10.4	9.72	3.06	2370	2.51
4	2.54	6.5	2.64	8.45	10.4	17.1	1.95	4160	1.82
5	2.55	6.3	7.72	23.8	10.4	36.6	(1)	8970	1.58
6	2.54	2.9	1.14	1.63	10.4	3.26	5.13	800	1.93
7	2.56	3.1	1.30	1.95	10.4	4.30	4.84	1060	2.48
8	2.55	3.3	1.73	2.80	10.4	6.31	4.25	1550	3.03
9	2.54	3.5	7.62	13.1	10.4	38.1	(1)	9300	0.80
10	1.27	12.6	7.62	47.2	10.4	38.1	(1)	4640	1.43
11	1.26	5.9	1.11	3.19	10.4	3.96	3.96	478	0.99
12	1.27	6.4	1.26	3.97	10.4	5.03	3.89	614	1.66
13	1.26	6.7	1.74	5.68	10.4	7.44	3.03	900	2.20
14	1.27	6.4	2.64	8.30	10.4	12.7	1.80	1540	1.67
15	1.27	7.0	7.43	25.5	10.4	28.6	(1)	3500	1.37
16	3.81	4.5	1.17	2.57	10.4	4.39	4.59	1610	3.02
17	3.86	4.2	1.26	2.60	10.4	5.15	4.29	1920	3.13
18	3.76	1.8	1.21	1.08	10.4	3.02	5.78	1080	3.08
19	3.84	2.1	1.28	1.33	10.4	4.11	5.48	1520	2.63
20	3.18	5.1	2.62	6.58	8.4	15.9	2.58	6010	2.06
21	2.03	8.3	1.73	6.99	8.4	10.5	3.12	2560	2.17
22	3.18	5.1	2.62	6.58	10.5	15.4	2.49	4660	2.77
23	2.03	8.3	1.73	6.99	10.5	10.4	3.02	2030	2.20
24	3.18	5.1	2.62	6.58	12.6	15.2	2.51	3850	2.23
25	2.03	8.3	1.73	6.99	12.6	10.6	3.06	1730	2.11
26	3.18	5.1	2.62	6.58	15.1	16.6	2.19	3490	1.88
27	2.03	8.3	1.73	6.99	15.1	11.1	2.87	1500	1.95
28	3.18	5.1	2.62	6.58	7.1	16.4	2.17	7290	1.94
29	2.03	8.3	1.73	6.99	7.1	10.4	3.16	2990	2.21

TABLE III (Continued)

Test No.	dx10(cm)	$t/dx10^2$	ρ_2(g/cm^3)	I*x10^3	νx10^3(cm^2/sec)	U(cm/sec)	nd/Ux10	Re	C_D
30	2.53	6.6	1.14	3.71	6.7	4.66	4.45	1760	2.14
31	2.57	6.2	1.30	3.98	6.7	5.82	4.29	2240	2.81
32	2.54	6.9	1.69	5.73	6.7	9.54	3.30	3620	2.61
33	2.54	6.5	2.64	8.45	6.7	17.6	1.97	6670	1.72
34	2.53	6.6	1.14	3.71	8.4	4.91	4.20	1480	1.94
35	2.57	6.2	1.30	3.98	8.4	6.00	4.19	1840	2.64
36	2.54	6.9	1.69	5.73	8.4	9.72	3.36	2950	2.51
37	2.54	6.5	2.64	8.45	8.4	17.0	1.90	5140	1.85
38	2.53	6.6	1.14	3.71	10.5	5.09	4.03	1230	1.80
39	2.57	6.2	1.30	3.98	10.5	6.31	4.07	1530	2.39
40	2.54	6.9	1.69	5.73	10.5	9.85	3.33	2380	2.46
41	2.54	6.5	2.64	8.45	10.5	17.6	2.01	4250	1.72
42	2.53	6.6	1.14	3.71	12.7	5.36	4.02	1070	1.62
43	2.57	6.2	1.30	3.98	12.7	6.50	3.97	1380	2.26
44	2.54	6.9	1.69	5.73	12.7	10.2	3.29	2040	2.31
45	2.54	6.5	2.64	8.45	12.7	17.3	1.98	3460	1.79
46	2.53	6.6	1.14	3.71	15.0	5.43	4.02	918	1.58
47	2.57	6.2	1.30	3.98	15.0	6.68	3.93	1150	2.14
48	2.54	6.9	1.69	5.73	15.0	10.5	3.12	1780	2.15
49	2.54	6.5	2.64	8.45	15.0	17.9	1.98	3040	1.66
50	1.26	6.7	1.74	5.68	12.8	7.75	3.40	766	2.03
51	1.26	6.7	1.74	5.68	8.8	7.53	3.17	1080	2.15
52	1.26	6.7	1.74	5.68	9.8	7.71	3.21	995	2.05
53	1.26	6.7	1.74	5.68	7.0	7.04	3.40	1270	2.46
54	1.27	6.4	2.64	8.30	12.8	14.6	1.73	1450	1.22
55	1.27	6.4	2.64	8.30	8.8	13.6	1.64	1970	1.41
56	1.27	6.4	2.64	8.30	9.8	13.8	1.71	1790	1.37
57	1.27	6.4	2.64	8.30	7.0	14.4	1.66	2630	1.25
58	3.81	6.3	1.26	3.86	18.8	5.73	4.16	2500	3.64
59	3.81	6.3	1.26	3.86	11.3	5.79	4.17	1960	3.56
60	3.81	6.3	1.26	3.86	13.8	5.79	4.09	1600	3.56

TABLE III (Concluded)

Test No.	dx10(cm)	t/dx10^2	ρ_2(g/cm^3)	I*x10^3	νx10^3(cm^2/sec)	U(cm/sec)	nd/Ux10	Re	C_D
61	3.81	6.3	1.26	3.86	9.8	5.85	4.02	2290	3.49
62	3.81	6.3	1.26	3.86	7.0	5.58	3.81	3030	3.84
63	3.81	6.3	1.32	4.07	8.8	7.65	4.17	3340	2.58
64	3.81	6.3	1.32	4.07	11.3	7.53	4.10	2550	2.66
65	3.81	6.3	1.32	4.07	13.8	7.74	4.02	2140	2.52
66	3.81	6.3	1.32	4.07	7.0	7.40	4.16	4050	2.75
67	11.4 (2)	1.6	1.18	0.90	9.8	3.60	6.39	4210	4.82
68	15.2 (2)	1.1	1.17	0.64	9.8	3.51	6.04	5480	4.70
69	20.3 (2)	0.38	1.01	0.19	9.8	1.43	8.74	3160	(3)
70	22.9 (2)	0.76	1.19	0.44	9.8	3.48	8.38	7930	5.67
71	30.5 (2)	0.52	1.20	0.30	9.8	3.23	9.62	10,100	5.76
72	17.8 (2)	1.3	1.37	0.84	9.8	5.64	6.18	10,270	5.09
73	7.62	2.1		48.0 (4)	165.0 (5)	43.3	(1)	2000	
74	29.9	2.39	0.026	26.6	165.0 (5)	104.8	(1)	19,000	2.74

(1) Tumbling motion
(2) Tested in towing tank
(3) Disk weight inaccurate
(4) I, measured directly
(5) Tested in air, $\rho = 1.15 \times 10^{-3}$ (g/cm)

3. DESCRIPTION OF THE DISK MOTION AND FLOW FIELD

The detailed motion and flow field of freely falling disks at very low Reynolds numbers is well documented in the literature. We will describe the sequence of events as the Reynolds number of the falling disk increases and supplement the discussion with results from the literature and from our investigation.

A. FLOW AT VERY LOW REYNOLDS NUMBERS (Stokes Flow)

At very low Reynolds numbers, $Re = Ud/\nu$, where U is the speed of fall, d is the disk diameter, and ν the kinematic viscosity, Schmiedel[8] observed that a disk will fall vertically with the same orientation that it had initially. Gans[11] has shown that at low Reynolds numbers where creeping motion obtains there is no aerodynamic moment produced by fluid pressure on a body that has three mutually perpendicular planes of symmetry. Schmiedel[8] mentions that experiments in this range are very difficult because it was not easy to orient the disks initially with their faces horizontal but gives no data about the Reynolds number range in which this motion was found. Squires and Squires[12] investigated the sedimentation of thin disks at very low Reynolds number but did not mention the range of Reynolds number in which a disk will maintain its initial orientation. Examination of their tabulated data on the drag of disks falling with their faces parallel and normal to the direction of motion shows that no drag measurements for disks falling edge on (with the face parallel to the direction of motion) were reported above a Reynolds number of 0.39. We have not investigated in detail the boundary below which the disk attitude depends only on the initial orientation. On one occasion we observed a vertical fall of a disk with its face parallel to the vertical at Re = 1.9. We attempted to repeat the experiment but the disk fell repeatedly at a light angle to the vertical and hit the side of the container. The Reynolds number in this case was also 1.9.

It is certain that a Reynolds number of the order of one marks the upper limit of the Reynolds number range in which the disk falls vertically and maintains its initial orientation.

B. STEADY LAMINAR FLOW ABOVE Re = 1

When the Reynolds number is greater than approximately one but less than approximately 100, a disk can be released with any initial orientation and will adjust itself to a horizontal attitude. The disk will then fall vertically and steadily with its face normal to the direction of motion. In this Reynolds number range the drag coefficient is already different from the Stokes flow result for creeping motion computed by Oberbeck[2] but lies below the drag computed by Oseen[3] in which the approximate effect of the inertial forces are considered. We believe that the inertial forces of the fluid are responsible for the tendency of the disk to fall face down. In this connection Schmiedel[8] mentions Kirchoff's

proof[13] that the fluid pressure on an ellipsoid of revolution in translational motion in an ideal fluid produces a torque which vanishes only when the ellipsoid moves in the direction of one of the three principal axes. Of these three possible equilibrium states of motion Kirchoff showed that only motion in the direction of the smallest axis is absolutely stable. The thin disk is the limiting case of an ellipsoid of revolution and Kirchoff's result suggests the reason for the observed orientation and stable motion of the disk in spite of the fact that the viscous flow about the disk and in the wake is hardly that of an ideal fluid.

The steady motion and flow field about the disk were observed visually and photographs of the interesting features are shown in Figures 1, 2, 3, and 4. The disks were painted with a concentrated solution of aniline dye* and allowed to dry before they were dropped in the water.

In Figure 1, a steadily falling disk is shown. The wake is perfectly straight after the initial oscillation ceases. The dark region behind the disk contains fluid in rotational motion that has passed near the disk and has carried away dye from the surface. A close up picture of the slowly rotating fluid in the wake is shown in Figure 2. The circular streaks are caused by inhomogeneities in the rotating dyed fluid which is in the shape of a distorted torus. Stanton and Marshall[5] mention that in 1877 Reynolds first pointed out the existence of the vortex ring behind a circular disk. A very small fraction of the dyed fluid in the vortex ring is deposited in the thread-like wake. The features of this steady flow field are quite similar to the steady flow behind spheres[8] or behind drops of liquid falling through a less dense liquid.[14]

When the disk reaches the bottom of the container and stops it releases the vorticity carried by the fluid behind the disk. Figures 3 and 4 show the details of the release. The released vorticity takes the form of a vortex ring that is connected to the front of the disk by a thin axisymmetric sheet of dyed fluid. In the photographs, Figure 3 and 4, the optical image of the disk and vortex ring are formed by reflected light from the lower side of the container.

We have measured the steady drag coefficient of the disks

$$C_D = \frac{\text{weight-bouyant force}}{\frac{1}{2}\rho_1 U^2 \pi r^2} \quad , \qquad (1)$$

where ρ_1 is the fluid density, U is the terminal velocity, and r is the disk radius. The drag coefficients in the Reynolds number range $1 < Re < 105$ are compared with the measurements of Schmiedel[8] in Figure 5. We have obtained good agreement with Schmiedel's results and can conclude that our simple experimental methods give satisfactory accuracy. Schmiedel[8] also considered the influence of the container wall

*Methyl blue chloride, Allied Chemical and Dye Corporation.

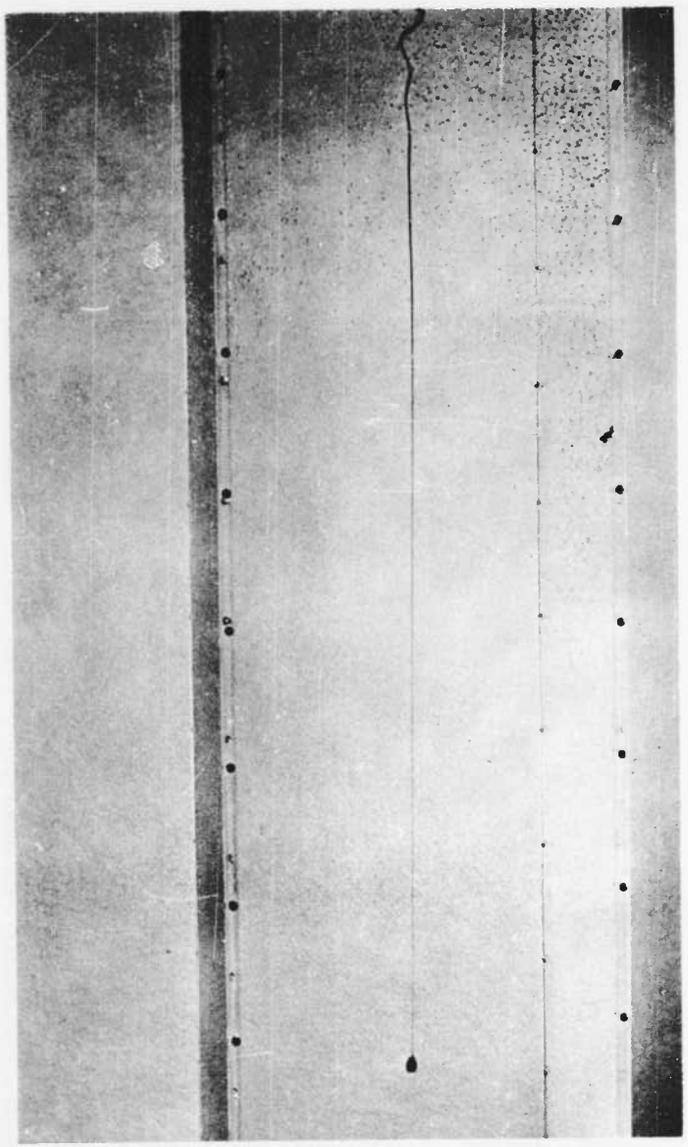

Figure 1. Vertical descent of a stable Plexiglas disk in water. Disk diameter 0.637 cm, disk thickness 0.0407 cm, Re ≐ 100. The black screw heads along the sides of the container are 10.2 cm apart.

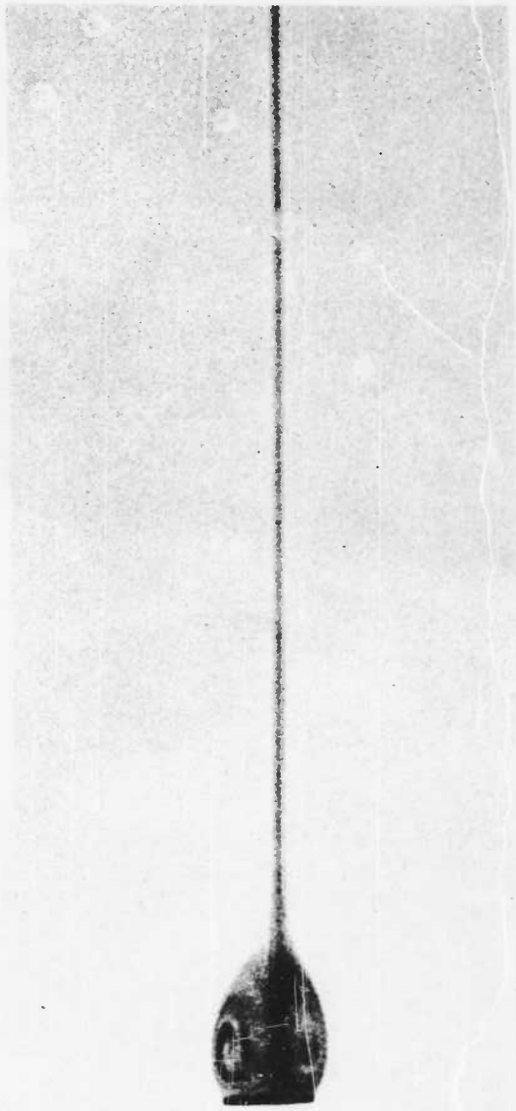

Figure 2. Flow field in the wake of a stable disk, same conditions as Figure 1.

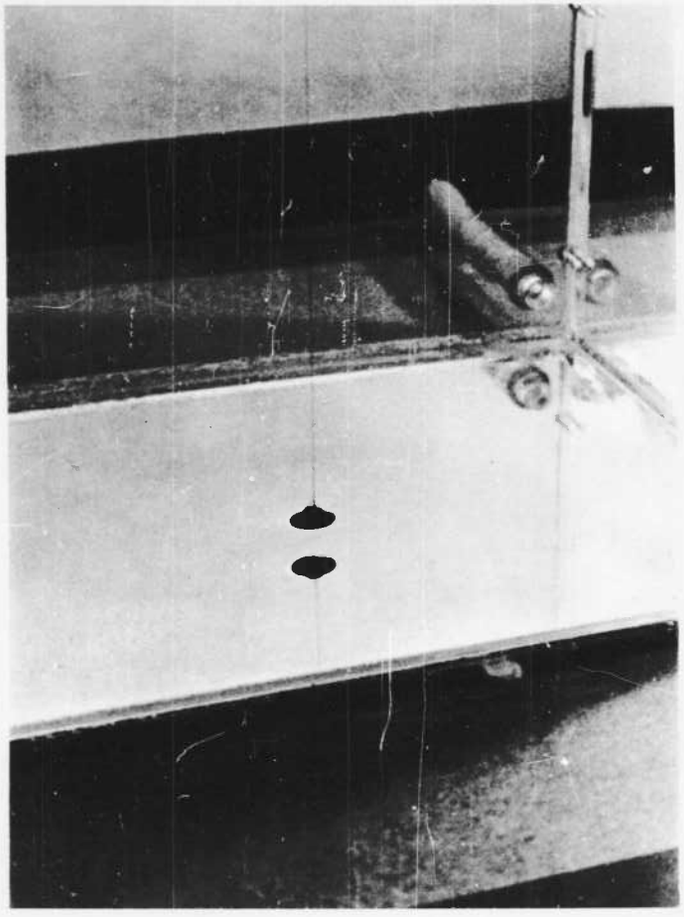

Figure 3. Release of vorticity from the wake of the disk of Figure 1 after stopping at the bottom of the container.

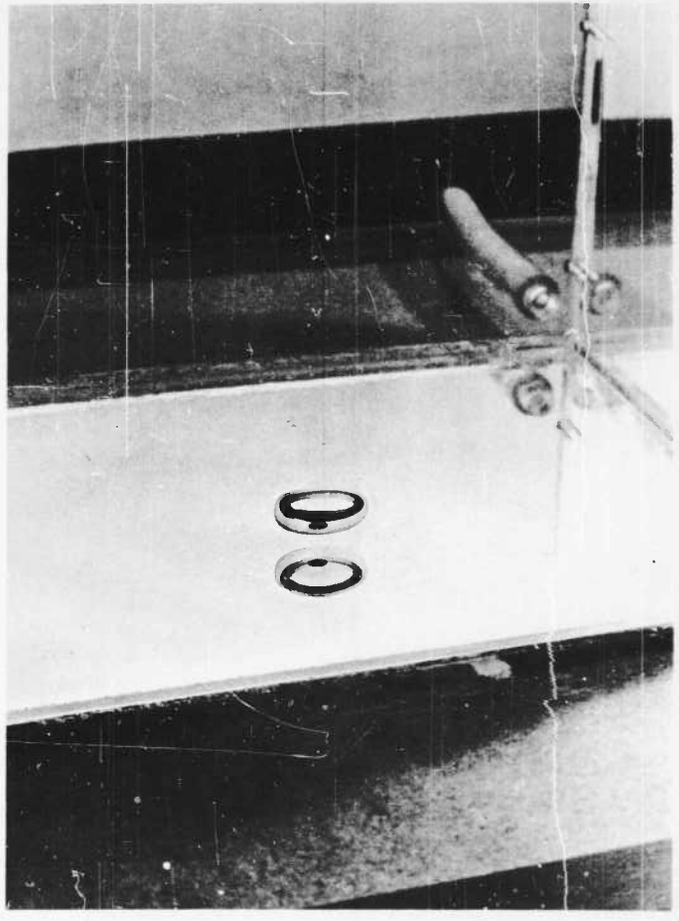

Figure 4. Vortex ring formed after release of vorticity from the wake of the disk of Figure 1.

on his drag coefficients and concluded that the influence was small. We have used almost the same diameter container in relation to disk diameter that Schmiedel used and can also state that the wall influenced the drag by no more than a few percent.

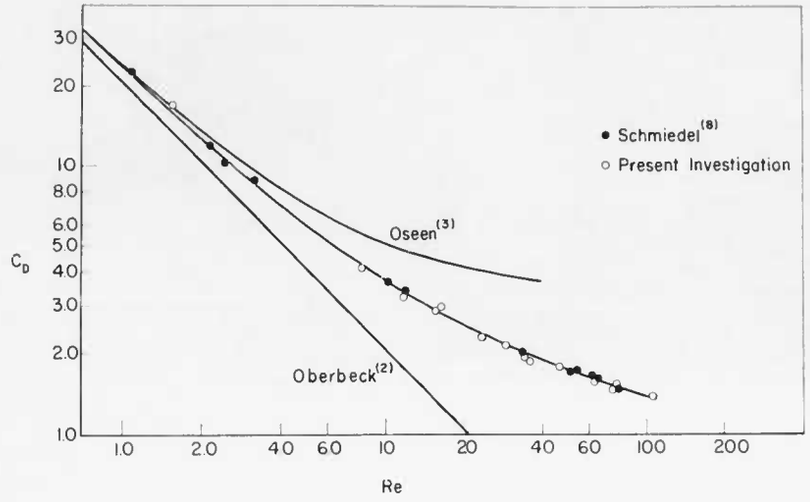

Figure 5. Drag coefficient as a function of Reynolds number for thin disks in steady motion.

C. DAMPED PITCHING OSCILLATIONS

In the Reynolds numbers range from approximately 1 to 100 damped pitching oscillations of the disk about a diameter were sometimes observed, see Figure 6. These oscillations remind one of Kirchoff's[13] integration of the complete equations of motion for the case of a solid of revolution that moves through an ideal fluid with its axis confined to one plane. Kirchoff showed that regular pitching oscillations of the solid can occur about an axis normal to the plane of motion. The oscillations could be excited by inhomogeneities in the fluid or by disturbances of the initial attitude when the disk was released. Evidence of damped oscillations caused by improper initial conditions can be observed in the wake trail at the top of Figure 1. Figure 7 shows that random excitation of oscillations caused by the disk falling at the same Reynolds number as Figure 1, through a medium that was not at rest. Whenever the disk oscillates or is disturbed during its fall it releases a horseshow shaped loop of vorticity that is connected by a vortex sheet to the dyed fluid immediately behind the disk. Rosenhead, in an appendix to Stanton and Marshalls report,[5] discusses the reason that horseshoe shaped vortex loops are observed when an axisymmetric wake is disturbed. The discussion relies upon the impossibility of a helical discharge of vorticity, Jeffreys;[15] and the known instability of axisymmetric sheaths or rings of vorticity.

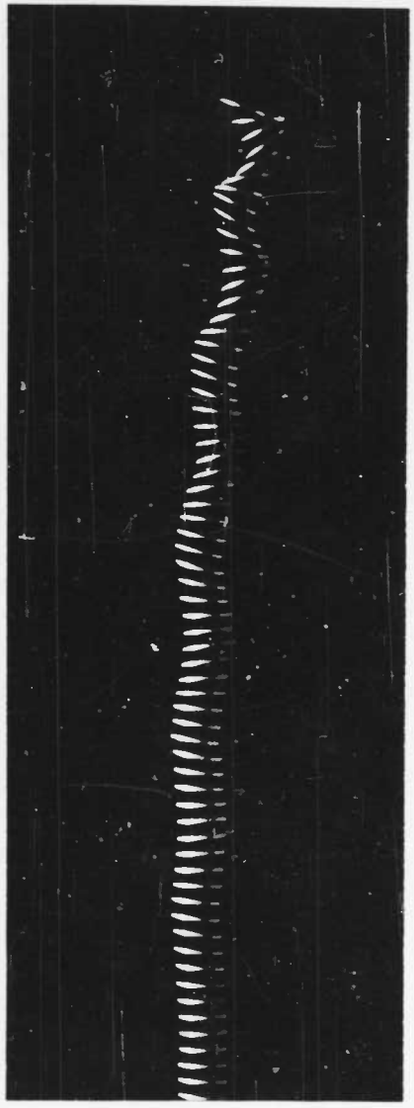

Figure 6. Stroboscopic picture showing the damping of the transient oscillatory motion of a Plexiglas disk in distilled water Repetition rate approximately 11/sec, disk diameter = 0.637 cm, disk thickness = 0.0504 cm, Re ≐ 100.

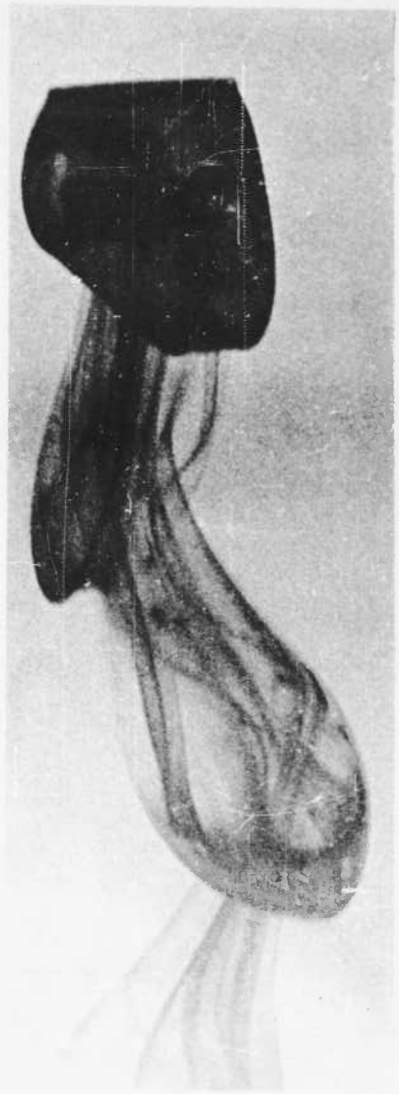

Figure 7. Vertical descent of a stable Plexiglas disk in a disturbed medium (agitated water) showing horseshoe shaped vortex loops released when disturbances are encountered.

The damping of the pitching oscillations was very great at low Reynolds numbers and decreased monotonically as the Reynolds number increased until at Reynolds number of the order of 100 the damping was very small. When the damping was very large the disk could be released with any desired inclination to the horizontal and would immediately assume a horizontal face down attitude without oscillating. At higher Reynolds numbers damped pitching oscillations were observed. The pitching oscillation was confined to a vertical plane normal to the diameter about which the disk first oscillated. Detailed observations of the frequency of oscillation and the amount of damping were not made in the Reynolds number range below Re = 100.

D. BOUNDARY BETWEEN STABLE AND UNSTABLE PITCHING OSCILLATIONS

When the Reynolds number was greater than 100 we observed that many of the disks were unstable. Small pitching oscillations about a diameter with little translational motion of the center of mass (see Figure 6 for example) increased in amplitude until appreciable translational motion of the center of mass in a vertical plane normal to the diameter defining the pitching oscillation was observed. Once established, the larger amplitude motion was quite periodic and regular and would persist until the disk reached the bottom of the container. On the other hand some disks, made of different materials or with different dimensions, exhibited only damped pitching oscillations which resulted in a steady descent at the same Reynolds number. We have investigated the boundary between the stable and unstable oscillations as a function of the dimensionless parameters pertinent to the phenomena.

The variables governing the phenomena are the fluid density, ρ_1, the disk density, ρ_2, the average speed of fall, U, the disk diameter, d, the disk thickness, t, and the fluid viscosity, μ. From these six dimensional quantities three independent dimensionless numbers may be formed among which will be obtained a functional relation governing the stability problem.

The three dimensionless numbers chosen are the dimensionless moment of inertia of the disk

$$I^* = \frac{I}{\rho_1 d^5} = \frac{\pi \rho_2 t}{64 \rho_1 d} , \qquad (2)$$

formed from the ratio of the moment of inertia of a thin disk about a diameter and a quantity proportional to the moment of inertia of a rigid sphere of fluid about its diameter, d, the Reynolds number,

$$Re = \frac{\rho_1 U d}{\mu} , \qquad (3)$$

and the thickness ratio of the disk,

$$\tau = \frac{t}{d} \quad . \tag{4}$$

This choice of dimensionless numbers was made in an attempt to separate the purely geometric effect of the disk thickness on the fluid flow from the dynamic or inertial effect of the disk thickness. The thickness of the disk will always enter as an inertial effect through the dimensionless moment of inertia, I*, which will affect the pitching motion. But, if the thickness ratio, τ, is small disks of different thickness should not have appreciably different aerodynamic characteristics.

We have made numerous observations of the motion of thin disks falling in solutions of glycerol and distilled water to locate the boundary separating the damped stable motion of the disk from the unstable motion that occurred for $Re > 100$. All but one of the disks used for these tests were made from steel shim stock as described in Section 2. The thickness ratio, τ, of the steel disks was always less than 0.04. One disk, test 16, Table II, was made from Plexiglas and tested in distilled water.

The experiment was very simple. The disks were dropped in quiescent liquid and the motion was observed. The results of the tests are shown in Table II, and Figure 8. If the amplitude of disk oscillation increased it was recorded as unstable, U. If the amplitude of oscillation was damped and the oscillations ceased before the disk reached the bottom of the container it was recorded as stable, S. If the oscillation was visibly damped but so slowly that it did not stop oscillating before reaching the bottom of the 120 cm high container it was recorded as, SO, but was considered to be stable. If the disk oscillation amplitude appeared to be constant it was labeled, B, for boundary. Each test with each disk was run a number of times in doubtful cases until the issue; S, SO, B, or U, was decided by the type of motion that appeared most frequently. For larger I*, $I^* > 2 \times 10^{-3}$, the decision S, SO, B, or U was easy to make. When I* was smaller $I^* < 2 \times 10^{-3}$ the decision became progressively more difficult. As I* was reduced more tests of the same disk had to be made until the issue was decided. Our points at the lowest I*, $I^* = 3.37 \times 10^{-4}$, did not present any difficulty compared to the greater scatter in the results of each test found near the peak maximum stable Reynolds number, at $I^* = 7.5 \times 10^{-4}$.

For determination of points near the boundary it was always necessary to use the 120 cm high container because the motion was sometimes only very slightly damped. It was often necessary to allow the liquid to come to rest for about an hour after stirring. We made special tests and found that we could always repeat our results near the stability boundary if we allowed the liquid to remain at rest for an hour or more after stirring. On one occasion we found a combination of disk and fluid in which the disk was observed to be very slightly unstable with very slowly increasing amplitude of oscillation. We covered the

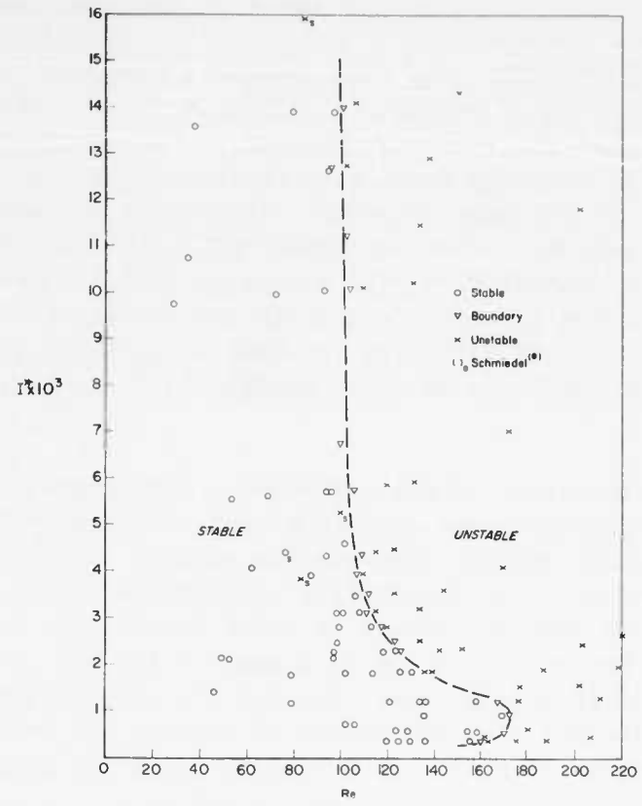

Figure 8. Dimensionless moment of inertia, I*, as a function of Reynolds number near the boundary separating stable and unstable oscillations of thin freely falling disks.

liquid and allowed it to settle over a weekend. When the test was repeated two days later the results were the same. We are confident that no destabilizing effects of disturbances in the fluid were overlooked. We did not find any effect of wall interference on these tests and were able to reproduce our results in either a small or large diameter container. The only influence of the walls that we noticed was a tendency for disk oscillations to cease when the disk was approximately one diameter from the bottom of the container.

The results of the stability tests, shown on the plot of Figure 8, can be compared with the work of others. It was Schmiedel's[8] work that stimulated our investigation. He reported steady disk motion below Re ≐ 80 for all his disks which were made from gold, silver, and steel. However, we had found very early that a relatively thick Plexiglas disk, with low I*, exhibited steady motion at a Reynolds number of 183 and began to investigate the stability problem.

We found, in the literature, the paper of Stanton and Marshall[5] who were quoted by Simmons and Dewey[6] to have observed the onset of wake oscillations behind a disk mounted in a small water channel at Re = 195. However, in their

own tests, Simmons and Dewey reported the onset of wake oscillations behind a disk with the same thickness ratio, $\tau = 0.1$, mounted in a wind tunnel at Re $\doteq$ 100. Upon reading Stanton and Marshalls paper it developed that their water channel was so narrow that the flow was practically a fully developed laminar pipe flow. Simmons and Dewey overlooked the fact that Stanton and Marshall mention that they have almost a parabolic velocity profile in their channel and, in addition, base their Reynolds number on the mean velocity. It is easy to understand the discrepancy between the results of the two investigations if we recall that the vorticity in a laminar channel flow will always be opposite in sense of rotation to the vorticity generated by a disk placed in the center of the channel. This, then, explains why sufficient vorticity for wake instability cannot be generated in the presence of the parabolic velocity profile until higher Reynolds numbers are attained.

We decided that the cause of the unexplained difference between Schmiedel's work, Simmons and Deweys work, and our first tests which gave Reynolds numbers for steady motion of 80, 100, and 183 respectively resided in the inertial forces produced by the disk motion. This supposition is confirmed by our results, Figure 8, on the variation of the Reynolds number at which instability occurs as a function of I*. For large I* the relatively large moment of inertia of the disk causes it to behave almost as if it were a fixed disk and the instability of motion begins at Re = 100 which coincides with the result of Simmons and Dewey[6] for a disk mounted in a wind tunnel. When I* is reduced the Reynolds number of the stability boundary increases and reaches a maximum value at Re = 172 and $I^* = 8 \times 10^{-4}$. We believe that the increase in the Reynolds number for the onset of unstable motion with decreasing I*, is caused by a favorable coupling between the disk pitching motion and the generation, distortion, and motion of the vorticity behind the disk. The tendency toward non-uniform vortex generation and shedding at the edge of the disk is probably reduced by the pitching motions of the disk but we have not attempted to construct a model to describe this effect. We are presently investigating the phase relationship between the position, aerodynamic torque, and vortex shedding of a large disk undergoing forced oscillations in a wind tunnel. We hope to gain a better understanding of the mechanisms which control the disk stability and motion from these tests.

We have not been able to definitely explain the lower value of Re = 80 that Schmiedel[8] found for oscillation of his disks. We can mention three possible reasons for the discrepancy: First, Schmiedel's disks were of larger thickness ratio, $0.007 < \tau < 0.02$, than the disks that we used, $0.004 < \tau < 0.008$, for our tests of the location of the stability boundary, Table II. Second, Schmiedel may not have allowed his liquid to come completely to rest before making his tests. Thirdly, Schmiedel observed oscillations on movie film over the central third of a 40 cm high container and may not have noticed slightly damped oscillations.

E. REGULAR PITCHING AND TRANSLATIONAL OSCILLATIONS

The motion of the falling disks in the unstable region at Reynolds numbers greater than those on the boundary for stable motion was investigated in some detail. In the unstable region the most common type of motion that was observed was a simple extension of the pitching motion with little translational motion of the disk, that was observed near the boundary, to a pitching motion of larger amplitude accompanied by a translational motion of the disk in a plane normal to the pitching axis. The translational motion was usually confined to one plane and was periodic. A definite frequency could be assigned to the oscillation in every case in which the translational motion was confined to a vertical plane. A slight rotation of the plane of translational motion about a vertical axis was sometimes observed. The frequency of oscillation, speed of descent, and amplitude of motion were always the same as the case of no rotation. A definite spiral motion of the disk about a vertical axis was sometimes observed if the surface normal to the disk face did not lie in a vertical plane when the disk was released or if the disk met a disturbance in the fluid as it fell. The spiral motion was irregular and difficult to repeat. The irregularity of the motion prevented any quantative measurements of the frequency of rotation, speed of descent or amplitude of the spiral motion. We have discarded the tests in which spiral motion occurred.

We have found that the unsteady wake of a disk executing small amplitude oscillations near the boundary for stable motion is laminar and contains two rows of staggered, equally spaced horseshoe shaped vortex loops on either side of the wake. When the intensity of the vorticity in the horseshoe shaped vortex loops is relatively large the loops break away from the wake and form a staggered array of two rows of closed vortex rings. An example of this type of wake is shown in Figure 9. The pattern is very similar to that observed by Magarvey and Bishop[14] behind non-oscillating drops of liquid above a certain critical Reynolds number.

Figure 10 shows some features of the flow field at a relatively high Reynolds number in the wake of disk in the case of regular pitching oscillations of large amplitude. This motion was first photographed and described by Schmiedel.[8] From the wake flow of Figure 10, it appears that the disk flies in curved descending arcs carrying with it bound vorticity and releasing a vortex at the extremes of the motion. The released vortices are connected to each other by two trailing vortices from the edges of the disk, the flow in the wake usually appeared to be turbulent.

Within this mode of oscillation there appeared a considerable variation in the frequency of the oscillation and the amplitude of the translational and pitching motion. When the disks had a large moment of inertia in comparison to a given volume of liquid, large I*, the pitching amplitude, frequency of oscillation, and falling speed were large and the amplitude of translational motion was small. When the moment of inertia was reduced, I* small, the pitching amplitude, frequency of oscillation and falling speed were small and the amplitude of translational motion became very large. The disks often encountered the sides of the

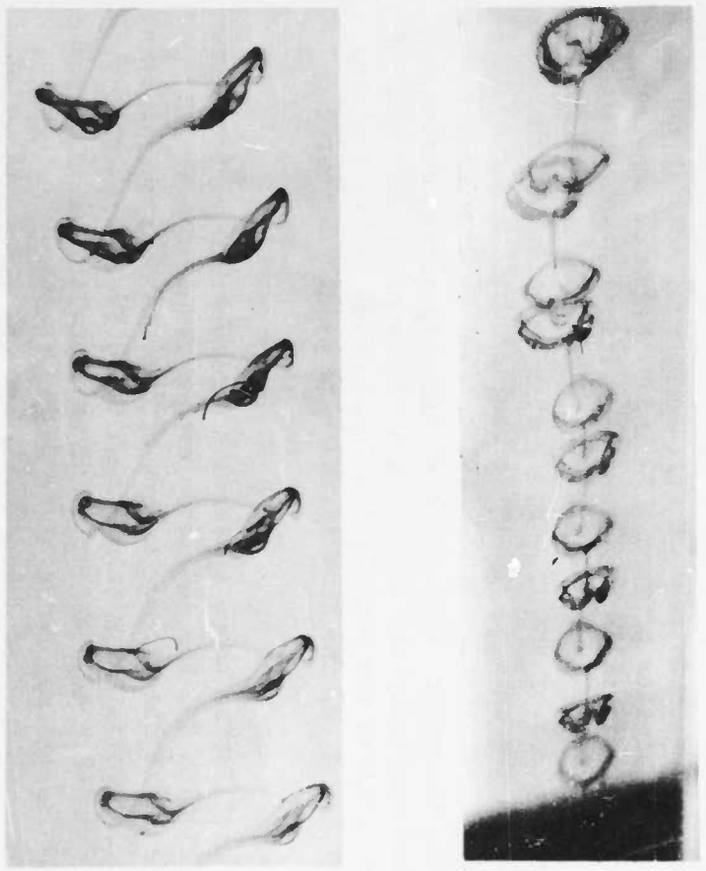

(a) (b)

Figure 9. Staggered arrangement of two rows of equally spaced (5 cm) vortex rings left in the wake 40 sec after passage of a disk that exhibited oscillatory pitching motion as it fell almost vertically, Re = 170; (a) View normal to plane of oscillation. (b) View with camera 60 cm to the right in the plane of oscillation near the top of (a).

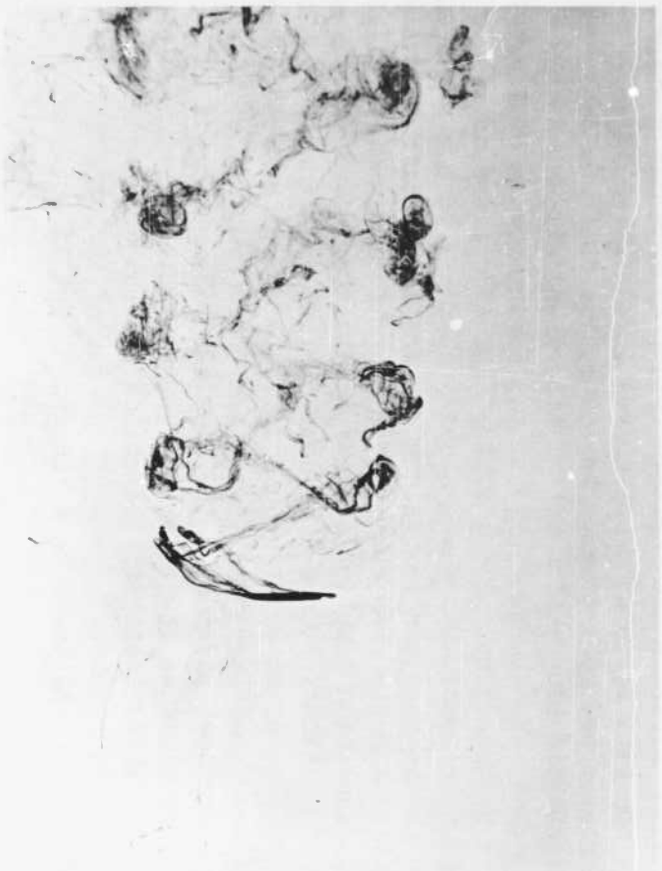

Figure 10. Wake of a freely falling disk that exhibited regular translational and pitching oscillations. Test No. 8 of Table III; Re = 1547, $I^* = 2.80 \times 10^{-3}$, nd/U = 0.43.

container when I* was small. We were fortunate to be allowed access to The University of Michigan ship model towing tank for free fall tests of large plastic disks at a time when the tank water had not been agitated for a few days. We found large amplitude oscillations, typically of the order of a meter for tests 67 to 72 of Table III. On one occasion we tested a polystyrene disk of 1 ft diam with I* = 1.24×10^{-4}. The amplitude was so large that the disk glided slowly out of view down the tank and we did not see it again. In this type of motion the slow oscillations were seldom confined to a single vertical plane because the disks were very sensitive to disturbances at the extremes of their motion which often caused a slight change in the attitude of the disk and resulted in a slight rotation of the vertical plane of oscillation.

The data from tests in this mode of motion is collected in Table III. In the problem of disk oscillations the frequency, n, enters as a variable that must be added to the variables already discussed in the stability boundary investigation, Section 3D. Another dimensionless number, nd/U, the dimensionless frequency, is added to the previous dimensionless numbers I*, Re, and τ.

Using the same scheme as before we have found it possible to order the data of Table III on a plot, see Figure 11, of Reynolds number versus I* in which nd/U enters as a parameter. For this plot we also measured the frequency of oscillation of a few disks on the stability boundary. The data on the frequency of oscillation along the stability boundary are recorded in Figure 12. Using the data of Table

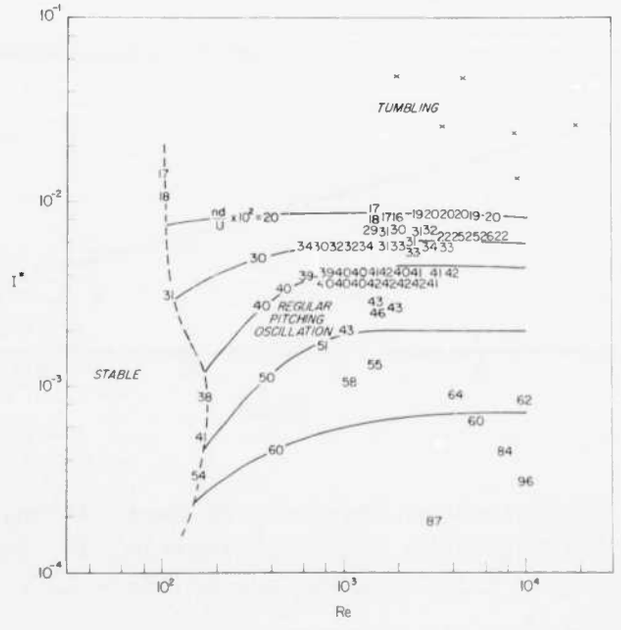

Figure 11. Map of the dimensionless moment of inertia, I*, and the Reynolds number for freely falling disks of Table III that exhibited regular pitching oscillations or tumbling motion. The numbers on the map indicate the location of each point and the magnitude of nd/Ux10^2.

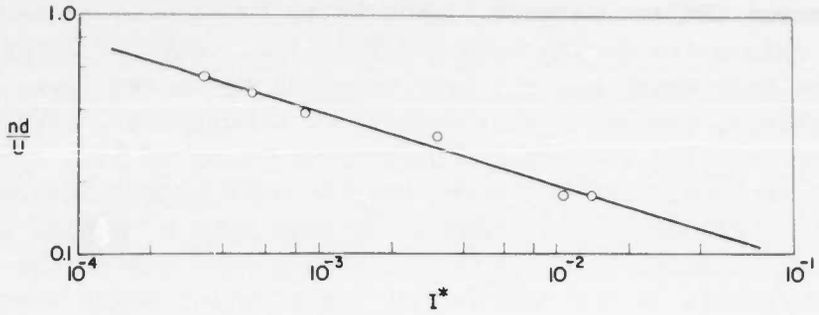

Figure 12. Dimensionless frequency of oscillation, nd/U, as a function of dimensionless moment of inertia, I*, along the boundary between stable and unstable pitching motion of freely falling disks.

III and Figure 12 we have labeled each point on Figure 11 with the measure value of the dimensionless frequency and sketched in curves of constant nd/U. At low Reynolds numbers the dimensionless frequency of oscillation, nd/U, depends on both I* and Re. At higher Reynolds numbers the dimensionless frequency, nd/U, becomes independent of Re. This is a behavior one might expect when viscous effects are confined to a thin boundary layer and the aerodynamic force and moment coefficients change only slowly with Reynolds number. At large Reynolds numbers, Re = 10^4, a cross plot from Figure 11 of nd/U versus I* reveals that there is an approximately linear relationship between I* and nd/U, see Figure 13. We have no explanation for this apparently simple behavior.

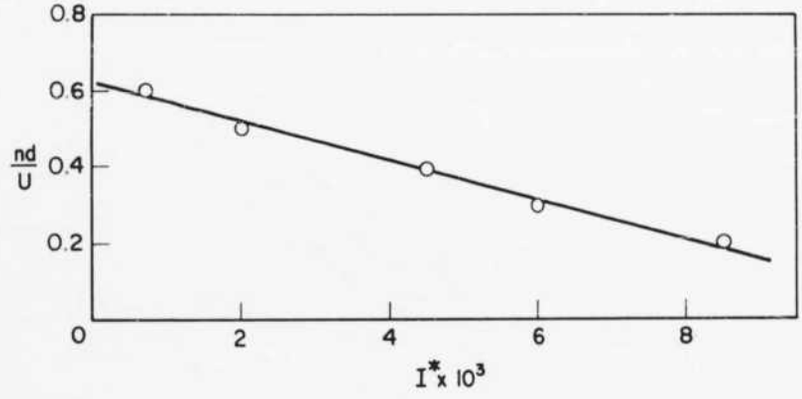

Figure 13. Dimensionless frequency of oscillation, nd/U, as a function of dimensionless moment of inertia, I*, for freely falling disks at a high Reynolds number, Re = 10^4.

We have used our data, Table III, to compute the weight of the disks when immersed in fluid. An average upward force coefficient, C_D, was defined and entered in Table III. The fluid mechanical meaning of this force coefficient is not of much interest because in each case the motion is different. A plot of C_D versus Re was made but the results showed a wide scatter. Schmiedel[8] also mentions that

his drag coefficient data were widely scattered in the region of regular oscillation.

We have not been able to include Schmiedel's[8] data on the dimensionless frequency of oscillating disks on our Figure 11. Schmiedel does not agree with our location for the stability boundary, Figure 8, and his dimensionless frequency is in general 40% higher than ours when R ≐ 250. Near the boundary for stable motion there is better agreement. The general behavior of nd/U with changes in I* and Re for Schmiedel's data is the same as we have found. It is also significant that Schmiedel's drag coefficients are much greater (twice as great) than we have measured in the range of Reynolds number and I*, where the disks oscillate. Schmiedel mentions that he tested a few aluminum disks whose dimensionless frequency of oscillation differed in an inconsistent way from his other observations. Unfortunately, he did not include this data in his paper.

We have noticed that the thickness ratio, τ, has some effect on the value of the dimensionless frequency, nd/U. The greatest discrepancy in nd/U for disks of different τ was found at Re ≐ 3000 and I* ≐ 6.5×10^{-3}. In this case, see Figure 11, the value of nd/U is increased by approximately 30% when τ is increased from 0.05 to 0.063. We also made a few tests with disks with sharp beveled edges. The location of the data on the plot of Figure 11 and the value of nd/U changed very little, but the speed of fall and frequency of oscillation were increased when the edge was beveled. We believe that our data for larger τ, display the general features of the dependence of nd/U on I* and Re but may differ somewhat if compared with results for smaller values of τ at the same Re and I*.

We have also noticed an effect of the container diameter on the dimensionless frequency of oscillation, nd/U. A number of disks were dropped in small containers and in the ship model towing tank. It was found that the value of nd/U was at most 15% higher for disks at large I* that exhibited large amplitude pitching oscillations and approached the wall of the small container at the extremes of the oscillation.

F. TUMBLING MOTION OF DISKS

When I* became larger the amplitude of pitching oscillation increased. We have observed a few tests with heavy metal disks falling in water that exhibit a tumbling motion. This type of motion can be observed when a coin is dropped in a pool of water. In this motion I* is of the order of 10^{-2} or greater. When the disk is released it may complete one or two oscillations of increasing pitching amplitude and then completely overturn on the next cycle. Once the disk has overturned it falls quite rapidly in an apparently random manner. The disks usually hit the container sides. Their ultimate location on the bottom of a large container could never be predicted. We also made a disk with a balsa wood frame covered with microfilm. When dropped in air, test 73, Table III, the value of I* was quite large and the disk tumbled. Another disk was made of styrofoam and dropped in air, test 74, Table III. It also had a large I* and tumbled. All

the tests in which the disks tumbled are shown by crosses on Figure 11. The lowest value of I^* for which we observed the tumbling motion was $I^* = 1.3 \times 10^{-2}$. We have not made any attempt to define the boundary for tumbling motion although no essential difficulty should be encountered.

Kirchoff's[13] result on the integral of the equations of motion for an ellipsoid of revolution in an ideal fluid also includes the case of complete revolutions (overturning) of the disk. However, in an ideal fluid one would not find a random dispersion of the disk at the bottom of the container and the motion would be confined to a vertical plane if given the proper initial conditions.

4. CONCLUSIONS

An orderly description of the gross features of the motion of freely falling disks has been given. The Reynolds number for instability of the wake behind a fixed disk has been shown to be 100 in agreement with the investigation of Simmons and Dewey.[6] In the region of unstable laminar wakes behind disks executing regular pitching oscillations we have observed a staggered array of regularly spaced closed vortex loops similar to the configuration observed by Magarvey and Bishop[14] behind drops of liquid. Some new results have been obtained on the relation between I* and Re along the boundary between stable and unstable motions of freely falling disks and on the relation between I*, Re, and nd/U for regular pitching oscillations. It should be possible to determine the relation between I* and Re along the boundary separating the tumbling motion and regular pitching oscillations of falling disks.

5. REFERENCES

1. S. Goldstein (editor) Modern Developments in Fluid Dynamics (Oxford Univ. Press, Oxford, 1938), Vol. 2, Chapter XIII.

2. A. Oberbeck, Crelles Jour. 81, 62 (1876)

3. C. W. Oseen, Arch. F. Math u. Phys. 24, 108 (1915).

4. Th. Von Karman, Gottinger Nachr. 509 (1911); 547 (1912).

5. T. E. Stanton and D. Marshall, A.R.C. British R. and M. No. 1358 (1930).

6. L.F.G.Simmons and N. S. Dewey, A.R.C. British R. and M. No. 1334 (1930).

7. A. Roshko, NACA Rep. 1191 (1954).

8. J. Schmiedel, Physik Z. 29, 594 (1928).

9. Bingham and Jackson, Bulletin Bu. Stds. 14, 75 (1918).

10. C. Hodgman (editor) Handbook of Chemistry and Physics (Chemical Rubber Publ. Co., Cleveland, 1960) 42nd edition pp. 2019 and 2212.

11. R. Gans, Münch, Berichte, S. 191 (1911).

12. L. Squires and W. Squires, Jr., Trans. Am. Inst. Chem. Engr. 33, 1 (1937).

13. Kirchoff, Crelles Jour. 71, 237 (1869) or H. Lamb, Hydrodynamics (Dover Publications, New York, 1945) 6th edition, Chapter VI, pp. 160-177.

14. R. H. Magarvey and R. L. Bishop, Phys. Fluids 4, 800 (1961) and Canadian Jour. Phys. 39, 1418 (1961).

15. H. Jeffreys, Proc. Roy. Soc. (London) A, 128, 376 (1930).